land

Article

NDVI-Based Vegetation Dynamics and Their Responses to Climate Change and Human Activities from 2000 to 2020 in Miaoling Karst Mountain Area, SW China

Yangyang Wu [1,2], Jinli Yang [3], Siliang Li [2], Chunzi Guo [2,4], Xiaodong Yang [3,5], Yue Xu [6], Fujun Yue [2], Haijun Peng [6], Yinchuan Chen [7], Lei Gu [8], Zhenghua Shi [3] and Guangjie Luo [1,9,*]

1   School of Geography and Resources, Guizhou Education University, Guiyang 550018, China; wuyangyang@gznc.edu.cn
2   School of Earth System Science, Tianjin University, Tianjin 300072, China
3   College of Ecology and Environment, Xinjiang University, Urumqi 830017, China
4   Administration of Ecology and Environment of Haihe River Basin and Beihai Sea Area, Ministry of Ecology and Environment of People's Republic of China, Tianjin 300061, China
5   Department of Geography and Spatial Information Techniques, Center for Land and Marine Spatial Utilization and Governance Research, Ningbo University, Ningbo 315211, China
6   State Key Laboratory of Environmental Geochemistry, Institute of Geochemistry, Chinese Academy of Sciences, Guiyang 550081, China
7   Shanghai Ecology and Environment Scientific Research Center, Yangtze River Basin Ecological Environment Supervision and Administration Bureau, Ministry of Ecology and Environment of People's Republic of China, Shanghai 200120, China
8   College of Geography and Remote Sensing Sciences, Xinjiang University, Urumqi 830017, China
9   Guizhou Provincial Key Laboratory of Geographic State Monitoring of Watershed, Guizhou Education University, Guiyang 550018, China
*   Correspondence: luoguangjie@gznc.edu.cn

Abstract: Understanding spatiotemporal shifts in vegetation and their climatic and anthropogenic regulatory factors can offer a crucial theoretical basis for environmental conservation and restoration. In this article, the normalized difference vegetation index (NDVI) of the Miaoling area from 2000 to 2020 is studied using a trend analysis and the Mann–Kendall mutation test (MK test) to review the vegetation's dynamic changes. Our study uses the Hurst index, a partial correlation analysis, and a geographic detector to investigate the contributions of climate change and human activities to regional vegetation changes and their drivers. We found that Miaoling's annual average NDVI was between 0.66 and 0.83 in 2000–2020, with a mean of 0.766. The overall trend was slow upward (0.0009/year), and 53.82% of the region continued to grow and gradually increased from west to east in the spatial domain, among which the karst regional NDVI distribution area and its growth rate were higher than those of non-karst sites. Based on correlations between climatic factors and NDVI, precipitation seasonality (coefficient of variation, CV) had the strongest correlation (positive correlation) with NDVI, while vapor pressure deficit (VPD) had a negative correlation with NDVI. In the interaction, human activities played a dominant role in the influence of NDVI on the vegetation of Miaoling. The night light index had the most explanatory power on the NDVI (q = 0.422), and the interaction between anthropogenic factors and other factors dominated its explanatory power. This study has academic and practical importance for the management, protection, and sustainable development of karst basins.

Keywords: vegetation dynamics; Miaoling; karst plateau; trend analysis; geographic detector

1. Introduction

Since the Anthropocene, human-induced global climate change has had a significant impact on terrestrial ecosystems [1]. As carbon, water, and energy exchangers between land and air, plants can provide people with oxygen, food, fiber, fuel, carbon sinks, and other

valuable ecosystem services [2–4]. Accordingly, significant changes in the global climate and their impacts on vegetation growth over recent decades have received increasing attention [5]. These include changes in climate and environmental conditions as well as human activities, such as land use change. Environmental factors include a wider range of chemical, physical, and biological elements that can affect ecosystems, including disturbances such as droughts, fires, and floods [6]. The normalized difference vegetation index (NDVI) is becoming a significant indicator in studying the spatial vegetation dynamics of regional ecological changes [7–9]. Thus, the role of climate and human factors in vegetation dynamics is one of the hottest topics in global change science [10,11].

The impact of climate change and human activity on vegetation change has been studied by many scientists. Research shows that climate change mainly impacts vegetation by changing climate, temperature, precipitation, soil moisture, and seasonal variations [7,10,12,13]. Amongst these, temperature controls the growth and distribution of vegetation by preventing the onset, termination, and distribution of the photosynthetic process [14,15], which is considered the main cause of the greening trend in northern latitudinal and elevated regions (Qinghai–Tibetan Plateau) [16–18]. However, in the middle and lower latitudes, temperature does not have an important impact on plant growth. However, precipitation has a clear role in boosting vegetation growth in arid and semi-arid regions [19,20]. For example, in southwest Chinese karsts [21,22] and Xinjiang [23], precipitation seasonality and variability significantly affect vegetation change. Precipitation, rather than temperature, has become the key factor controlling vegetation growth [20,24]. Soil moisture, which is strongly related to temperature and precipitation, has become an important limiting factor in arid and semi-arid areas. Furthermore, with high temperatures and heatwaves, the atmospheric vapor pressure deficit (VPD) is becoming an increasingly important driver of plant community function. High VPD can induce plant stomatal closure to prevent high water loss [25,26], which has been identified as a major factor in extreme drought-induced plant death [25]. Clearly, the impacts of climate change on vegetation cover are diverse and complex because of regional variations in climate change and ecological environmental conditions.

At present, vegetation changes and their spatial patterns are strongly affected by human activities. With the rapid development of the world's population and economy, the impact of anthropogenic activities on changes in surface vegetation cover is increasing, affecting the balance of terrestrial ecosystems on a large scale [8]. Among these, land use change is a significant and strongly spatially changing factor in vegetation change. On the one hand, unreasonable agricultural activities, excessive reclamation, grazing, and urban expansion significantly reduce vegetation cover [27,28]. On the other hand, human activities can increase vegetation cover by planting trees, closing hills to reforestation, and improving agricultural technology [29,30]. Besides land use change, many studies have used the night light index (NLI) to characterize regional economic development or urbanization and the intensity of surface human activities [29–31]. Therefore, the NLI was included as one of the factors influencing vegetation in the NDVI.

There are few studies on the connection between vegetation changes and their drivers in important watersheds in the karst region, although there have been many studies on the impact of climate variation and human behaviors on vegetation change [3,7,10,15,19,20]. Miaoling Mountain is an important watershed ecological security barrier in the karst region of southwest China. It is located in the center of the core area of southwest China's karst plateau. The contradiction between man and land is pronounced due to the high ecological sensitivity and vulnerability of karst areas, plus climatic factors. Biomass above ground [32,33] and biomass below ground [34,35] are significantly lower in karstic forests than in non-karstic forests. Therefore, vegetation plays an important role in managing karst desertification and restoring ecosystems [36]. However, to our knowledge, the driving mechanism of human activities on NDVI changes in vegetation in the Miaoling's karst watershed is still unclear; there is no research to quantify how climatic and human factors affect vegetation in the area. Additionally, the impact of each driver on vegetation change has not been quantified.

Based on this deficiency, this article aims to study the vegetation dynamics of important watersheds (Miaoling) in karst areas from the following four perspectives: climate, human activity, topography, and soil. The aims of this article are as follows: (1) to analyze the variation characteristics and trends of the NDVI's spatial distribution in Miaoling from 2000 to 2020; (2) to explore the correlation between climate factors and NDVI; and (3) to explore the key driving factors affecting the NDVI of Miaoling vegetation. The results of this study have far-reaching significance for the sustainable ecological development of karst areas in southwest China and the realization of China's strategic goal of "carbon peaking and carbon neutrality". At the same time, it provides a reference value for the vegetation's dynamic driving factors in the important karst watershed and theoretical guidance for ecological environment management and sustainable development of the watershed.

2. Materials and Methods

2.1. Study Area

Mt. Miaoling, the research site, is located in the center of the core region of the Karst Plateau in southwest China. It is an important watershed for the ecological security barrier of the watershed in the karst region of southwest China. Its main range (25.73°–27.16° N, 103.82°–109.48° E) takes the watershed of the Pearl River system and the Yangtze River system as the main axis and then extracts the Miaoling study area from the small watershed in the north and south of the main axis and divides it into east, central, and west sections (Figure 1). From east to west, Miaoling is the watershed of the Yuanjiang River Basin, the Liujiang River Basin, the Wujiang River Basin, the Hongshui River Basin, the Niulan-Jiang-Heng He River Basin, and the Beipanjiang River Basin. The altitude in the area is 146–2877 m, and the peaks are often above 1500–2000 m. The main peak of the eastern section is Leigong Mountain, at up to 2179 m. The middle section of Doupeng Mountain is 1961 m high, and the western section with Laowang Mountain is 2127 m above sea level. The eastern, central, and western parts reach an altitude of 2179 m. Miaoling is a humid, mountainous area with a sub-tropical monsoon climate. The main vegetation in the Miaoling Mountain area consists of mixed evergreen and mixed broadleaf forests as the primary forest type and shrubs, grass, and forbs as the vegetation degradation type, which differs significantly from the zonal non-karst vegetation of evergreen broadleaved forests in subtropical China (ECVC 1980) [37,38]. It is one of the important forest areas in Guizhou Province. Miaoling has no tectonic veins, and the geology and topography of the sections are very different. Additionally, it is formed by a number of north–south anticlines composed of hard rock formations and a combination of uplifted and high regions. The layered landforms composed of planes and large karst basins are the most prominent regional landforms, thus forming unique landscapes such as planes with concentrated arable, basin areas, and terraced fields located high on the hillsides.

2.2. Data

The NDVI is based on the Google Earth Engine cloud computing platform and selects US remote sensing imagery from the Landsat 5, Landsat 7, and Landsat 8 satellites with 16-day temporal resolution and 30 m spatial resolution. At the same time, the dataset was referenced by the Land Use and Global Change Remote Sensing Team of the Institute of Geographical Sciences and Natural Resources Research, Chinese Academy of Sciences, with a spatial resolution of 30 m and a temporal resolution of each year [39]. Through methods such as series data preprocessing and data smoothing, the maximum NDVI value of each pixel in a year from 2000 to 2020 was obtained. The annual mean NDVI values from 2000 to 2020 were generated using the maximum synthesis method (MSV). When generating long-time series NDVIs, the maximum value synthesis method can decrease the effect of cloud cover, shadows, suspended particles in the atmosphere, etc., so that the error is reduced and the accuracy is improved [39].
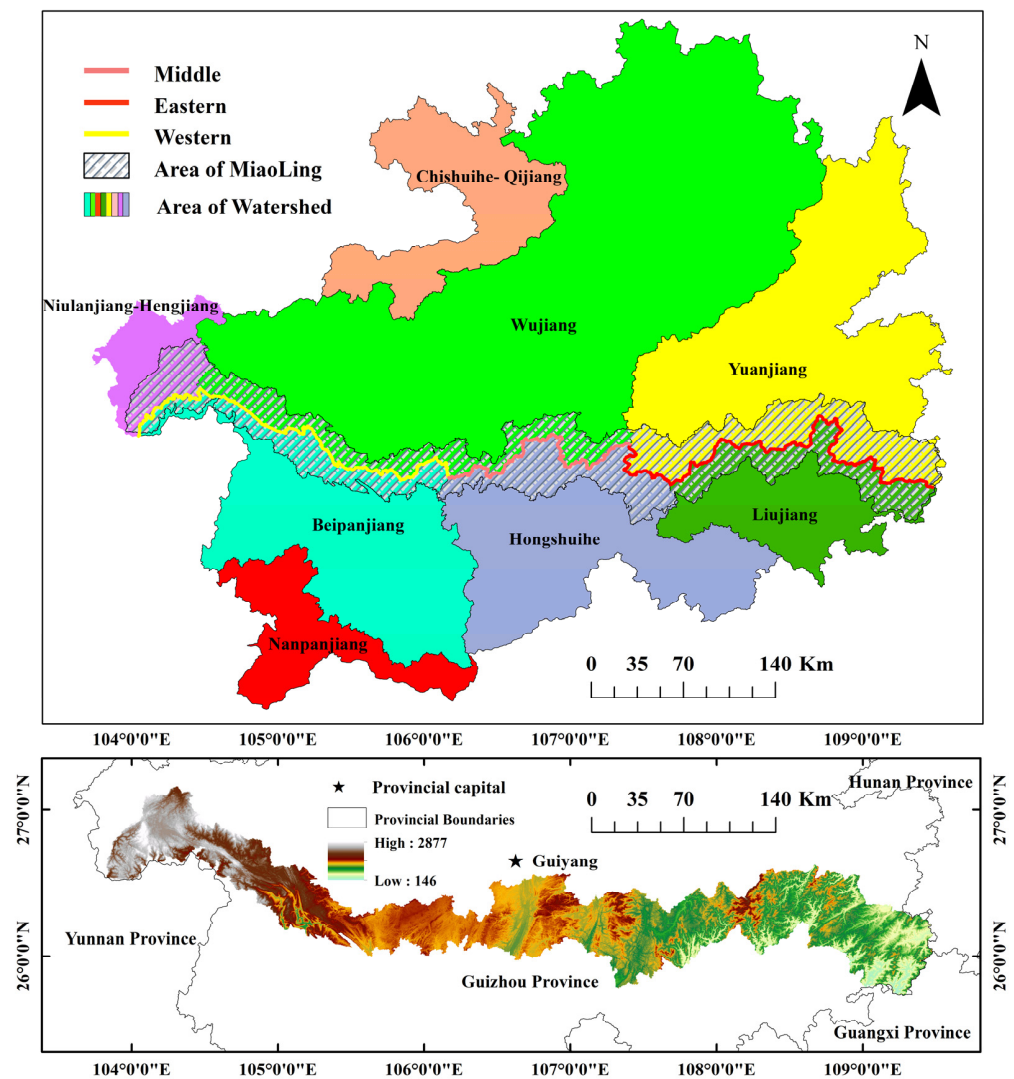
Figure 1. Location of the Miaoling Mountain area.

The DEM data involved in this study are derived from the geospatial data cloud, which is downloaded using a rectangular frame clipping area and then transformed into raster data through an ArcGIS overlay, which is the basis for the calculation of the total height, slope, and aspect of the research region. The land use change data are sourced from Zenodo (https://zenodo.org/, accessed on 15 June 2020) and published by Huang Xin et al. from Wuhan University in China [40]. The biggest advantage of this dataset is its continuous 30 m land use classification results. The NLI can be used to describe the intensity of human activity and is closely linked to economic development. This study selected it as a factor in human activity and conducted a related driving analysis.

The meteorological data use raster data for precipitation and air temperature with a resolution of 1 km. This dataset introduces the influence of terrain on the climate in the temperature and precipitation data generated by the ANUSPLIN interpolation tool. The interpolation error is the smallest, and the accuracy is greatly improved compared with other interpolation methods [41]. The analysis of meteorological elements is more suitable. The meteorological interpolation software ANUSPLIN is used to interpolate the data into monthly synthetic precipitation multi-band data with a spatial resolution of 1 km. It is highly accurate, has high resolution, is a long-time series, and has better scientific research and application potential [42]. The above-mentioned monthly synthetic temperature and precipitation data are extracted by ArcGIS and then resampled to 30 m.

Soil moisture is an important link between the atmosphere and the terrestrial ecosystem. The soil moisture data included a set of neural nets using a data fusion of up to 11 microwave remote sensing-based soil moisture products. These data were obtained by satellite for the global surface soil moisture for the period 2003–2018 with a spatial resolution of 0.1° [43]. The bioclimatic variable data are available at a spatial resolution of 1 km, with historical monthly weather data for 1960–2018 [44]. The range of data downloaded for this study was 2000–2018. The VPD dataset mixes the high spatial resolution climate normal of the Worldclim dataset with the less accurate but time-varying data from CRU Ts4.0 and Japan's 55-year reanalysis (JRA55) with climate-assisted interpolation. Conceptually, the interpolation time variation from CRU Ts4.0/JRA55 is often applied to Worldclim high spatial resolution climatology to create a high spatial resolution dataset covering a wider range of time records. The above data and the data sources involved in the study are as follows (Table 1):

Table 1. Data and sources.

Data Type	Factors	Time	URL
Vegetation	NDVI	2000–2020	https://code.earthengine.google.com
Climate	Precipitation seasonality(Coefficient of variation)	2000–2018	https://www.worldclim.org/data/
	Precipitation of wettest quarter	2000–2018	
	Mean annual precipitation	2000–2020	http://www.rescdc.cn
	Mean annual temperature	2000–2020	
	Vapor pressure deficit	2000–2020	https://climate.northwestknowledge.net/
Soil	Soil moisture	2003–2018	https://doi.org/10.1594/PANGAEA.912597
Landform	Elevation	2020	http://www.gscloud.cn/
Topography	Karst	2010	http://www.csdata.org/
	Non-karst	2010	
Human activity	Land use change	2000–2020	https://zenodo.org/
	Night light index	2000–2020	https://ngdc.noaa.gov/

2.3. Methods

In this study, in order to explore the characteristics, trends, and driving factors of vegetation change in Miaoling, we used the following methods to analyze the relevant data in sequence and with specific applications: We first conducted trend analysis and a Mann–Kendall (MK) trend test on NDVI changes in Miaoling's vegetation. Additionally, we used the Hurst index to perform a continuous analysis of the change trends of the NDVI to explore the continuity of the Miaoling NDVI trends in the spatial distribution and change trend. The correlation study of the regional distribution and variation trends of NDVI in Miaoling with climatic conditions was completed by using a partial correlation analysis. The association characteristics of the climatic elements, human activities, terrain, and vegetation changes in Miaoling were also studied using a geographic detector.

2.3.1. Theil–Sen Median Trend Analysis

We conducted a trend analysis on the NDVI of Miaoling's vegetation using the Theil–Sen median method, which is referenced in this literature [45] and is expressed in Equation (1) as follows:

$$\beta = \text{median}(\frac{x_j - x_i}{j - i}), \forall j > i \tag{1}$$

where j and i are the time series data. A value greater than 0 means that the time series shows an upward trend. A value less than 0 means that the time series shows a downward

trend, and a value closer to 0 means that the time series changes are not significant. The Theil–Sen median trend analysis and MK test significance test results were superimposed and analyzed. As Table 2 shows, the results are grouped into six categories. Based on the above results, we also conducted breakpoint detection on the dynamic trend of vegetation in Miaoling.

Table 2. Type of change trend of DNVI.

Slope	p	Trend	Slope	p	Trend
Slope < 0	$p < 0.01$	significant decrease	Slope > 0	$p < 0.01$	significant increase
Slope < 0	$0.01 < p < 0.05$	minimal decrease	Slope > 0	$0.01 < p < 0.05$	moderate increase
Slope < 0	$p > 0.05$	non-significant decrease	Slope > 0	$p > 0.05$	non-significant increase

2.3.2. Mann–Kendall Test

The Mann–Kendall trend test is a nonparametric statistical test used to test significant trends of change. The samples do not need to have a specific distribution, nor are they affected by a few outliers [46]. Equation (3) is as follows:

$$S_k = \sum_{i=1}^{k} \sum_{j=1}^{i} \text{sgn}(X_i - X_j)$$
$$UF_k = [S_k - E(S_k)]/\sqrt{\text{Var}(S_k)} \tag{2}$$

where X_i and X_j represent the NDVI values of time i and j, respectively. S_k is the cumulative count of $X_i > X_j$. $E(S_k)$ and $\text{Var}(S_k)$ are the mean and variance of S_k, respectively. $UF_k > 0$ indicates an upward trend of the NDVI sequence, while $UF_k < 0$ indicates a downward trend of the NDVI sequence. Combining the NDVI trend classification results (Table 2), the non-significant decrease and non-significant increase are classified into one category (i.e., no change). The results are divided into the following five levels [47]: significant decrease, moderate decrease, no change, moderate decrease, and significant decrease.

2.3.3. Hurst Index

The Hurst index is an effective method to describe the information dependence of long time series [48]. For the NDVI time series, NDVI (τ), = 1, 2, 3, 4, . . . , n. For any positive integer ≥ 1, the mean series of the time series is defined as follows:

$$\overline{\text{NDVI}}_{(\tau)} = \frac{1}{\tau} \sum_{t=1}^{\tau} \text{NDVI}_{(\tau)} \qquad \tau = 1, 2, \cdots, n \tag{3}$$

The Hurst index is calculated as follows:

$$\frac{R_{(\tau)}}{S_{(\tau)}} = (c\tau)^H \tag{4}$$

The relevant values involved in the calculation of the Hurst index are calculated as follows:
(1) The cumulative deviation is as follows:

$$X_{(t,\tau)} = \sum_{t=1}^{t} (\text{NDVI}_{(t)} - \overline{\text{NDVI}_{(\tau)}}), 1 \leqslant t \leqslant \tau \tag{5}$$

(2) The range sequence is as follows:

$$R_{(\tau)} = \max_{1 \leqslant t \leqslant \tau} X_{(t,\tau)} - \min_{1 \leqslant t \leqslant \tau} X_{(t,\tau)}, \tau = 1, 2, \cdots, n \tag{6}$$

(3) The standard difference order is as follows:

$$S_{(\tau)} = \left[\frac{1}{\tau}\sum_{t=1}^{\tau}(\mathrm{NDVI}_{(t)} - \mathrm{NDVI}_{\tau})^2\right]^{\frac{1}{2}}, \tau = 1, 2, \cdots, n \tag{7}$$

The Hurst index (value) may reflect the persistent nature of the NDVI time series. In the Hurst exponent (value), when $0 < H < 0.5$, this indicates that the change is continuing to decline, meaning that the future change trend is opposite to the past change trend. When $= 0.5$, this indicates that the NDVI time series is a random series and there is no long-term correlation. When $0.5 < H < 1$, the time series are characterized by long-term dependence and persistence, meaning that the future change is consistent with the past trend. In other words, areas that have tended to increase in past years are likely to increase in years to come, and vice versa. The closer it is to 1, the stronger the persistence.

2.3.4. Analysis of Correlation

To explore the response of vegetation dynamic changes in Miaoling to climate change factors, we conducted a partial correlation analysis between NDVI and climate factors (Table 3) to reveal the main driving forces controlling the interannual changes of NDVI from 2000 to 2020.

$$R_{12,3} = \frac{r_{12} - r_{13}r_{23}}{\sqrt{(1 - r_{13}^2)(1 - r_{23}^2)}} \tag{8}$$

where $R_{12,3}$, $R_{13,2}$, $R_{23,1}$ are the correlation coefficients among the variables; $R_{12,3}$ is the partial correlation coefficient between r_1 and r_2 after fixing the variable r_3. The value range of the partial correlation coefficient ranges from -1 to 1. When $R_{12,3} > 0$, the correlation is positive, meaning that both factors correlate in the same direction. When $R_{12,3} < 0$, the correlation is negative. The higher the partial correlation coefficient, the stronger the correlation between the two elements at the pixel.

Table 3. Statistics of the partial correlation coefficient and significance reveal the intricate relationship between climate factors and NDVI.

Factors	Mean	Correlation Coefficient Range	Extremely Significant Positive Correlation (%)	Significant Positive Correlation (%)	Non-Significant Correlation (%)	Significant Negative Correlation (%)	Extremely Significant Negative Correlation (%)
X1	0.32	−0.63~0.82	64.5	13	10.1	8.7	3.7
X2	−0.26	−0.68~0.76	11.4	7.5	9.2	17.2	54.7
X3	0.23	−0.57~0.66	23.6	34.6	16.9	18.7	6.2
X4	0.21	−0.67~0.79	49.2	5	17.7	19.1	9.1
X5	0.17	−0.58~0.66	40.2	13.5	15.1	14.2	17
X6	0.15	−0.59~0.65	15.3	32.2	25.4	12.5	15.3

Note: X1, precipitation seasonality (CV); X2, VPD; X3, precipitation of wettest quarter; X4, MAP; X5, soil moisture; X6, MAT.

2.3.5. Geographic Detector

Geographic detection is a new spatial statistical method to detect spatial differentiation and reveal driving factors [49]. It contains the following four detectors: factor detection, interaction detection, risk detection, and ecological detection. The first two parts apply here. The model is shown below:

(1) Factor detector

A factor detector could determine the effect of detecting the spatial heterogeneity of vegetation change. The spatial heterogeneity of X to Y could be expressed as $q \times 100\%$,

and the greater the number, the greater the influence of the detection factors on vegetation change [50], which is as follows:

$$q = 1 - \frac{\sum_{h=1}^{L} N_h \sigma_h^2}{N \sigma^2} \tag{9}$$

where h is the vegetation change or detection factor hierarchy; N is the number of class h or total region units; and Y is the change in class h or total region Y value.

(2) Interaction detector

The interaction detector is appropriate to identify the impact of the combination of the detection drivers X_a and X_b on the heterogeneity of the spatial variation of vegetation. The five interaction results are as follows: [50].

Miaoling's vegetation change trend from 2000 to 2020 was regarded as the dependent variable Y. The selected driving factors mainly include the key factors selected by partial correlation analysis as the detection factor X, as shown in Table 4.

Table 4. The q value of each driving factors.

Factors	X1	X2	X3	X4	X5	X6	X7	X8	X9	X10	X11	X12	X13
q value	0.355	0.322	0.243	0.21	0.17	0.155	0.272	0.173	0.125	0.331	0.401	0.397	0.422
p value	0.000	0.000	0.000	0.000	0.000	0.000	0.000	0.000	0.000	0.000	0.000	0.000	0.000

Note: X1, precipitation seasonality (CV); X2, VPD; X3, precipitation of wettest quarter; X4, MAP; X5, soil moisture; X6, MAT; X7, elevation; X8, slope; X9, aspect; X10, karst; X11, non-karst; X12, land use change; X13, NLI.

3. Results

3.1. Spatial Distribution and Trend Change of NDVI

This article uses a combination of the Theil–Sen test and the MK method, as well as breakpoint detection, to count pixels of vegetation coverage from 2000 to 2020. Research results show that Miaoling has a mean NDVI of 0.766 (Figure 2c). In addition, the average NDVI variation range of Miaoling over the years is 0.659–0.827, with a rising trend with an increase of 0.9×10^{-3}/year ($R^2 = 0.053$, $p > 0.05$) (Figure 2a). In addition, the breakpoint detection results indicate that there is a breakpoint in the Miaoling study time series (Figure 2b). As shown in Figure 2c, the change trend before and after 2011 was opposite. Before 2011, the NDVI in Miaoling showed an increasing trend, while it tended to decline after 2011. For the period 2000–2020, the overall NDVI in the Miaoling region slowly increased. However, there are significant fluctuations, mainly reflected in the sharp decline after 2010 and 2017 and the sharp growth in 2013. Especially after 2011 and 2018, the NDVI values tended to decrease, with a decrease rate of over 10% compared to the previous year's NDVI value in 2019.

The characteristics of the spatial distribution of the NDVI in Miaoling are shown in Figure 3. The eastern section is mainly characterized by a significant growth distribution of NDVI, accounting for 40.6% of the area. The NDVI in the middle segment mainly shows moderate growth, with an area ratio of 30.5%. The northern and western sections of the middle section are mainly characterized by a decrease and no change, with area proportions of 12.9% and 16%, respectively.
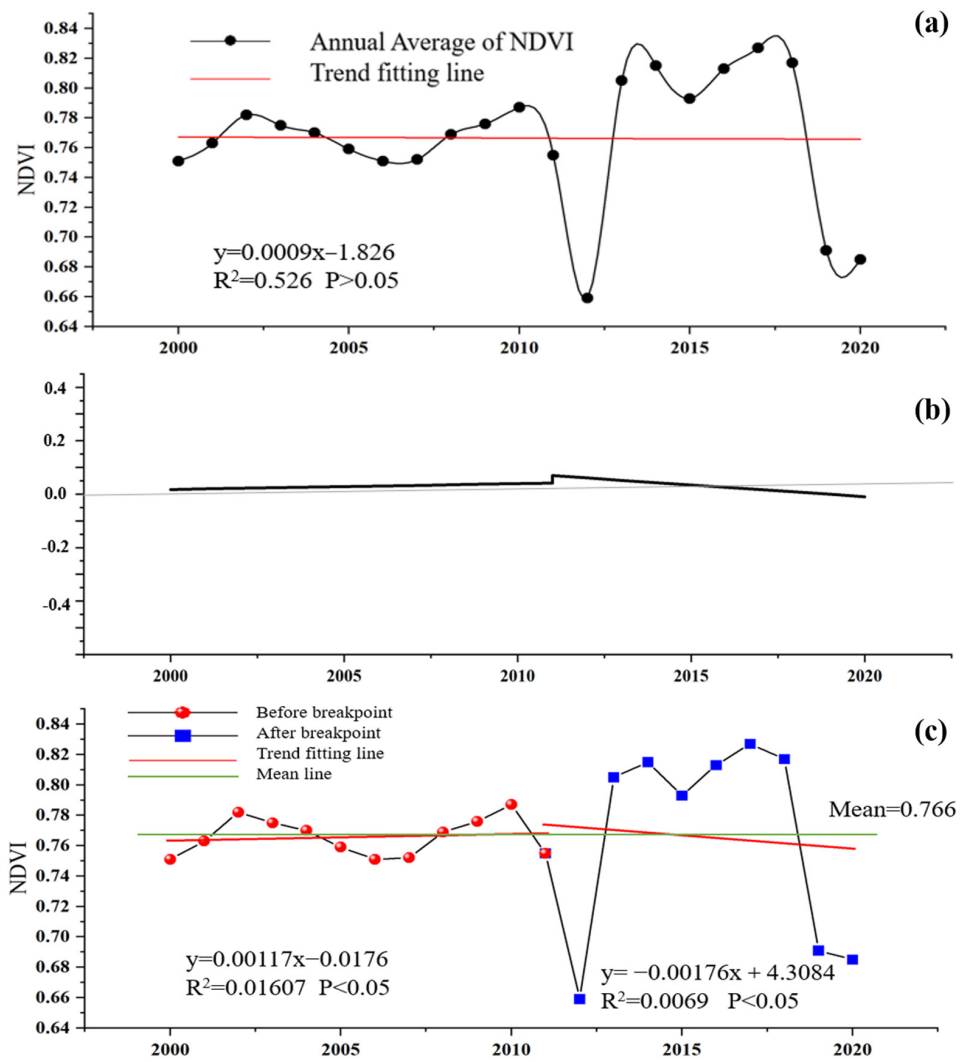
Figure 2. The variation characteristics of NDVI values in Miaoling from 2000 to 2020. (**a**) The interannual variation and trend fitting of NDVI values in Miaoling; (**b**) Breakpoint detection results; (**c**) Trend fitting of NDVI before and after breakpoints.
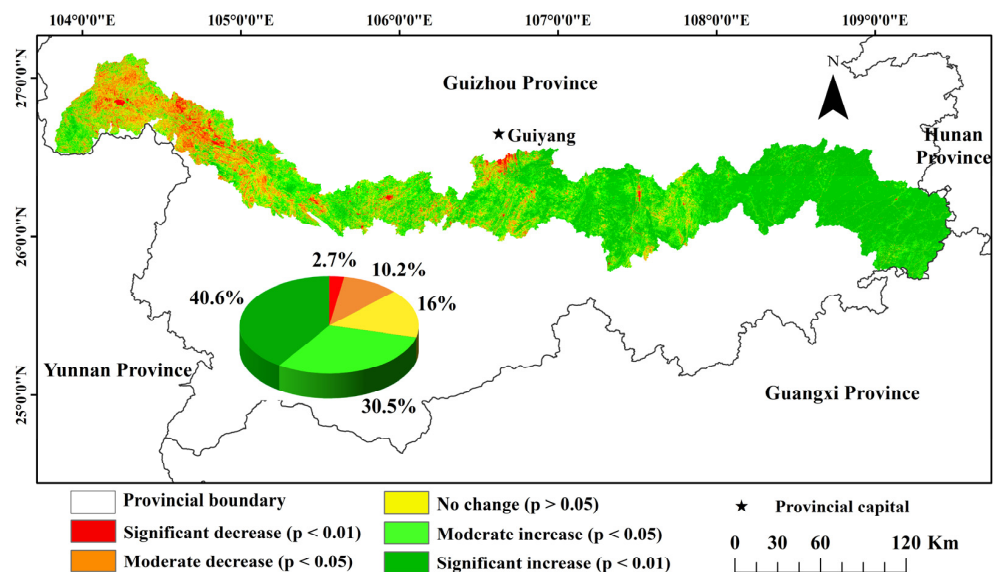

Figure 3. Distribution of the inter-annual NDVI in the Miaoling region from 2000 to 2020.

The annual average NDVI change can reflect the dynamic characteristics of vegetation and serve as an important indicator of vegetation health and ecosystem stability. Thus, the Theil–Sen median trend analysis was used to analyze the NDVI trend over the last 21 years at the pixel scale. We found that the spatial distribution of NDVI is highly heterogeneous (Figure 4a). The NDVI in Miaoling increased in most areas and decreased in some local areas. The change trend of NDVI in most areas is an increasing trend (accounting for 68.73%). Among them, the highest growth is concentrated in the east, accounting for about half of the total growth. In addition, the slightly degraded and significantly degraded areas account for 32.61%. The significantly degraded areas are mainly distributed in the western part of the study area. The remaining 8.66% did not show a significant change.
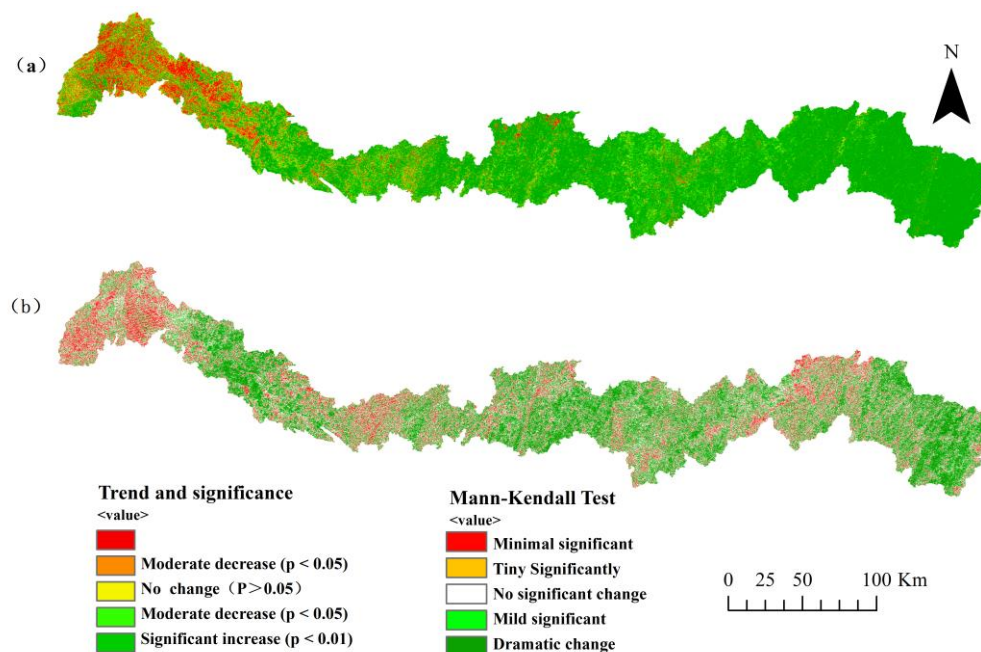

Figure 4. The trend of NDVI distribution (**a**) and MK test results (**b**) in the Miaoling area from 2000 to 2020. The results divide the change trend into five grades: significant degradation, $p < 0.01$; mild degradation, $p < 0.05$; no significant change, $p > 0.05$; mild improvement, $p < 0.01$; significant improvement, $p < 0.05$.

The MK test results indicate that from 2000–2020 (Figure 4b), the change in the NDVI in most areas of Miaoling is relatively strong, with a mainly strong distribution in the eastern, central–southern, and a small part of the western areas, while the area with an insignificant change is mainly distributed across the majority of the western Miaoling area.

We also tested the persistence of NDVI changes in Miaoling through the Hurst index, and the mean Hurst index of NDVI in Miaoling was found to be 0.56 (Figure 5). Additionally, the region with continuous growth ($0.5 < H < 1$) has the widest distribution (53.82%), mainly in the eastern and central parts of the study area. However, most of the west area is still trending down. As can be seen, the Hurst index of the NDVI has similar spatial heterogeneity to the distribution of the NDVI in the study area.

3.2. Impact Factor of Land Use Change on the NDVI

The karst area is mainly concentrated in the eastern and middle sections of the Miaoling area (Figure 6a), dominated by woodland and followed by grass. The non-karst area is mainly distributed in the western section and is mostly arable land, followed by grass (Figure 6b). The NDVI of the karst area is higher than that of the non-karst area in the Miaoling area.
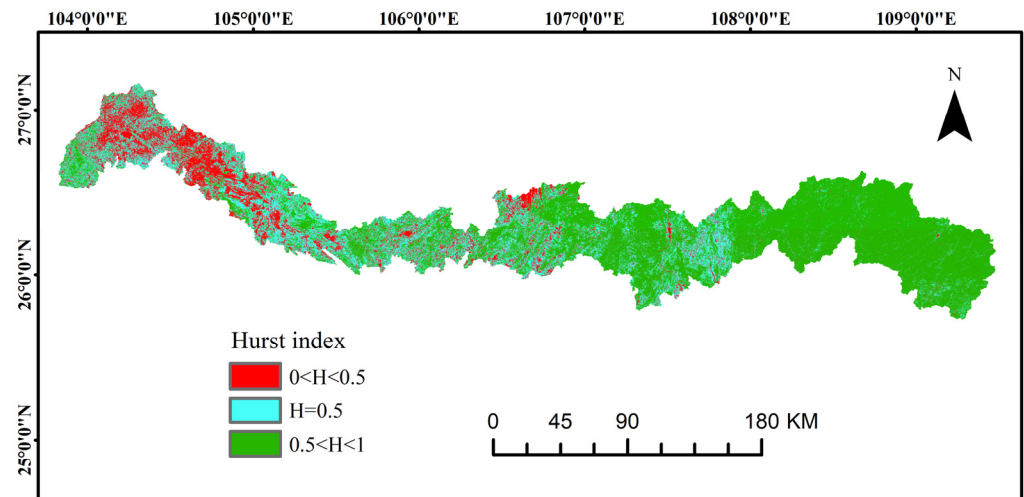
Figure 5. The Hurst index distribution of NDVI in Miaoling. 0 < H < 0.5; continuous decline; H = 0.5, no significant change; 0.5 < H < 1, continuous growth.
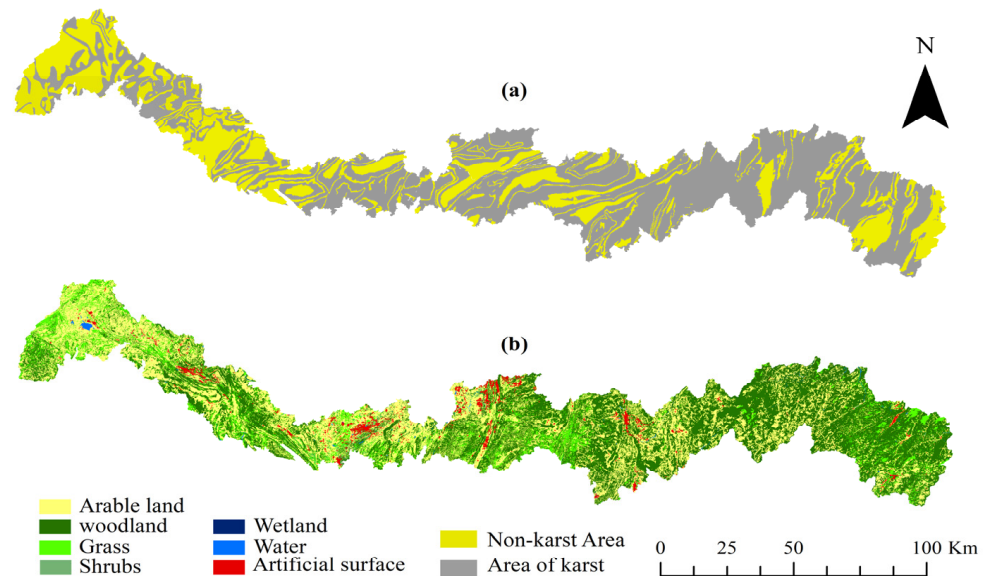

Figure 6. Karst distribution in Miaoling area of Guizhou Province (**a**) and spatial distribution characteristics of land use types (**b**) in 2000 to 2020.

The overall average proportion of land use types in the Miaoling area (Figure 7) is as follows: wood land (50%) > arable land (31.60%) > grass (14%) > artificial surface (1.93%) > shrub (1.45%) > waters (0.93%) > wetlands (0.09%). The total proportion of forest and arable land fluctuates, and the proportion of artificial surface continues to increase; grass, water, wetlands, and shrubs fluctuate slightly. Comparing the spatial distribution of NDVI in Miaoling (Figure 3) with land use types, it can be roughly divided into the following characteristics: The land use types corresponding to NDVI reduction areas are mainly concentrated in areas such as artificial surfaces, cultivated land, and wetlands. The NDVI of forested areas mainly manifests as growth.

The most immediate effect of land use change on NDVI is change. The most notable changes in NDVI are specifically in arable land and woods. Figure 8 shows that the Miaoling region's degraded regions of wood land, arable land, and grass are primarily located in the center region. As a result, it is clear from Figure 6b that the primary land use categories (wood land, grass, and arable land) in the Miaoling region are spread in regions with high concentrations of human activity (artificial surface areas).
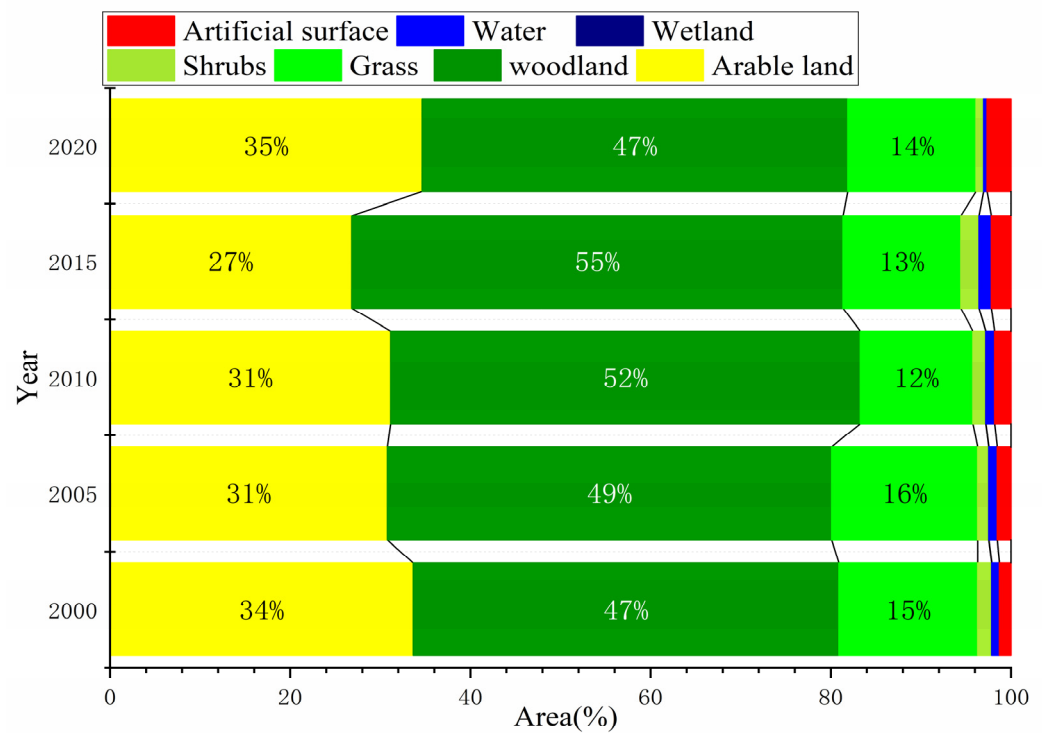
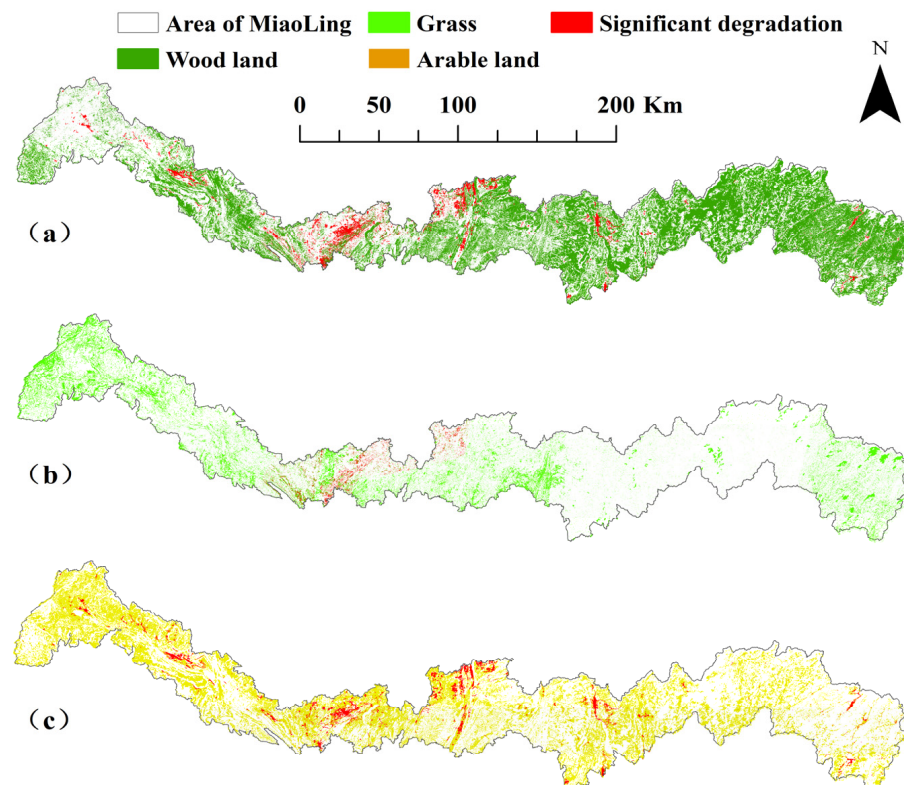**Figure 7.** Total area ratio of each land use type in Miaoling, Guizhou, from 2000 to 2020.

Figure 8. Woodland (**a**), grass (**b**), and arable land (**c**) change distribution characteristics in Miaoling.

3.3. Impact Climate Factors of the NDVI

　　Climatic factors are as important as human activities (land use change) in influencing vegetation dynamics. Our analysis of the partial correlation between NDVI and climate factors was calculated at the image metric scale for the studied region from the year 2000

to 2020. The findings of the partial correlation study make it clear that the NDVI and precipitation seasonality (CV) have the strongest association, whose mean correlation coefficient was 0.32. As shown in Table 3, their correlation strength is in order of precipitation seasonality (CV) (0.32) > VPD ($-$0.26) > precipitation in the wettest quarter (0.23) > MAP (0.21) > soil moisture (0.17) > MAT (0.15). The other five factors, with the exception of VPD, have an overall positive correlation with the NDVI.

The results showed significant spatial heterogeneity in the NDVI vegetation–climate correlation in the Miaoling region. In combination with Figure 9 and Table 3, 77.8% of the precipitation seasonality (CV) area was positively correlated with the NDVI (Figure 9a), which was widely distributed in the study area. A total of 71.9% of the VPD was significantly negatively correlated with the NDVI, and only 18.9% of the area was positively correlated with the NDVI, which was mainly distributed in the western and central parts of the study area (Figure 9b). A total of 58.2% of Precipitation of wettest quarter was significantly positively correlated with NDVI over the total area, and the areas with a significant negative correlation were mainly concentrated in the western part of the study area (Figure 9c). Precipitation was significantly positively correlated with NDVI in 54.2% of the spatial area and distributed in the westernmost, easternmost, and northernmost parts of the study area (Figure 9d). A total of 53.7% of the soil moisture area was significantly positively correlated with NDVI, while the easternmost area was significantly negatively correlated (Figure 9e). The least correlated climatic factor with NDVI in Miaoling was temperature, which was significantly positively correlated with NDVI in 47.5% of the study area, while MAT was significantly negatively correlated with NDVI in the far west and north (Figure 9f).
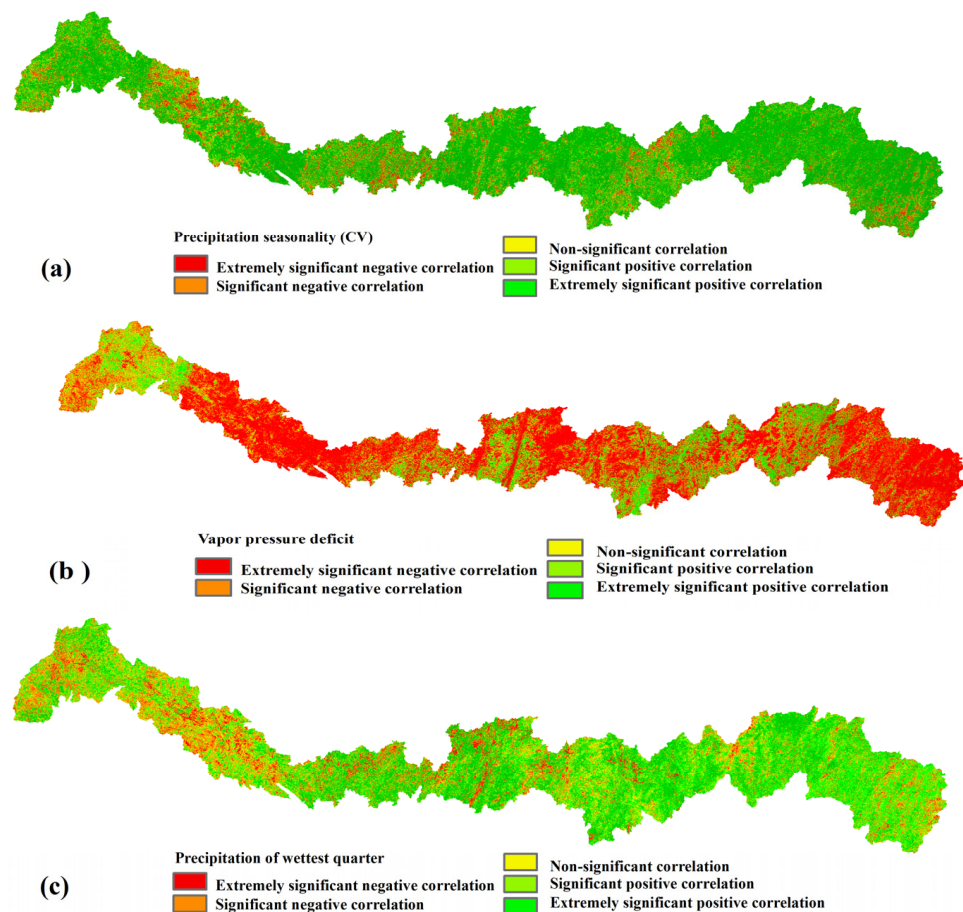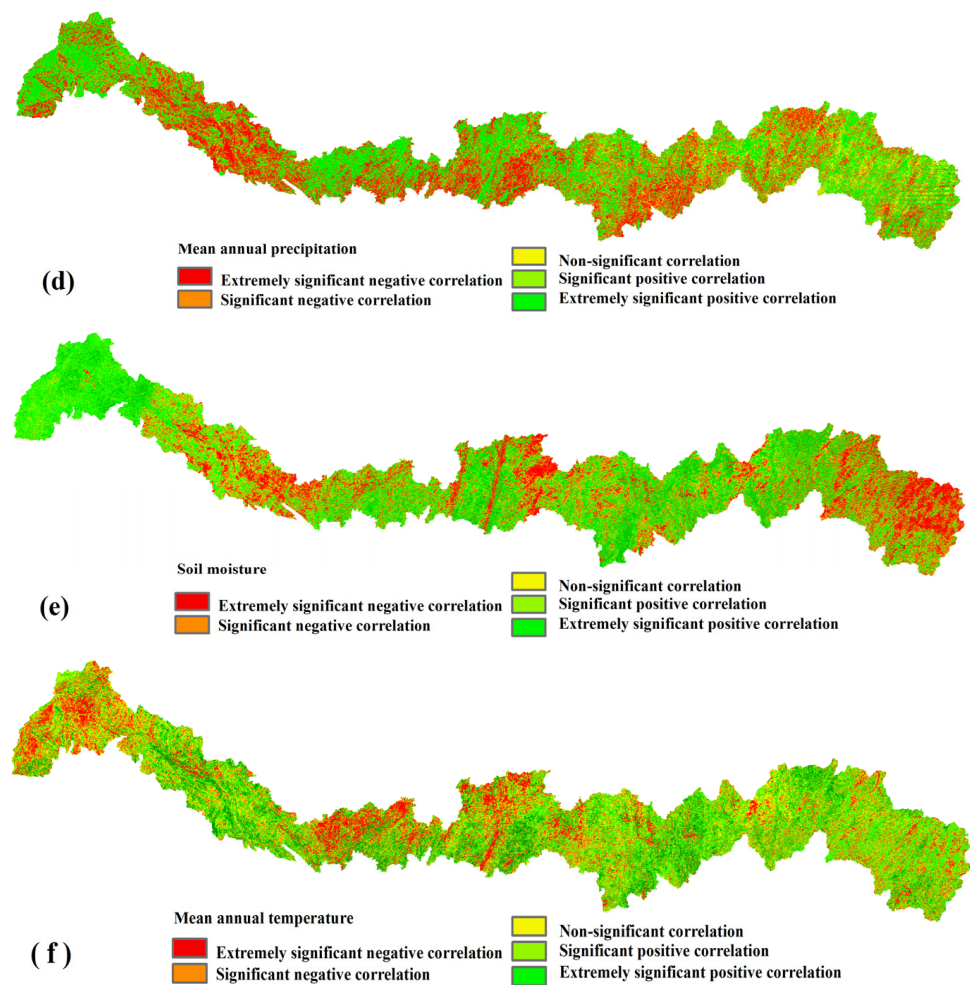

Figure 9. *Cont.*

Figure 9. Spatial distribution characteristics of partial correlation between NDVI in Miaoling and precipitation seasonality (CV) (**a**), VPD (**b**), precipitation of wettest quarter (**c**), MAP (**d**), soil moisture (**e**), and MAT (**f**).

In summary, precipitation seasonality (CV) and VPD in climate factors showed positive and negative related relationships with NDVI distribution and were all widely distributed across the study area, but the spatial heterogeneity of other climatic factors with NDVI was significantly complicated with them.

On the time scale, the average annual value of NDVI shows significant fluctuations in the study time series, but overall, it shows a slow growth trend (Figure 2a). The linear fitting trend of precipitation seasonality (CV) and the NDVI is upward (Figure 10a). Figure 10b shows that the NDVI value and precipitation seasonality (CV) have basically similar dynamic changes, and the NDVI increases and decreases with the increase and decrease in precipitation seasonality (CV). This result shows that precipitation seasonality (CV) has a positive effect on the increase and decrease in NDVI. On the contrary, the fitting trend of VPD and NDVI is decreasing (Figure 10c) because the general feature of VPD change is a significant upward trend, while the change of NDVI is contrary to the fluctuation of VPD. Therefore, it can also be concluded that there is a negative correlation between VPD and NDVI.
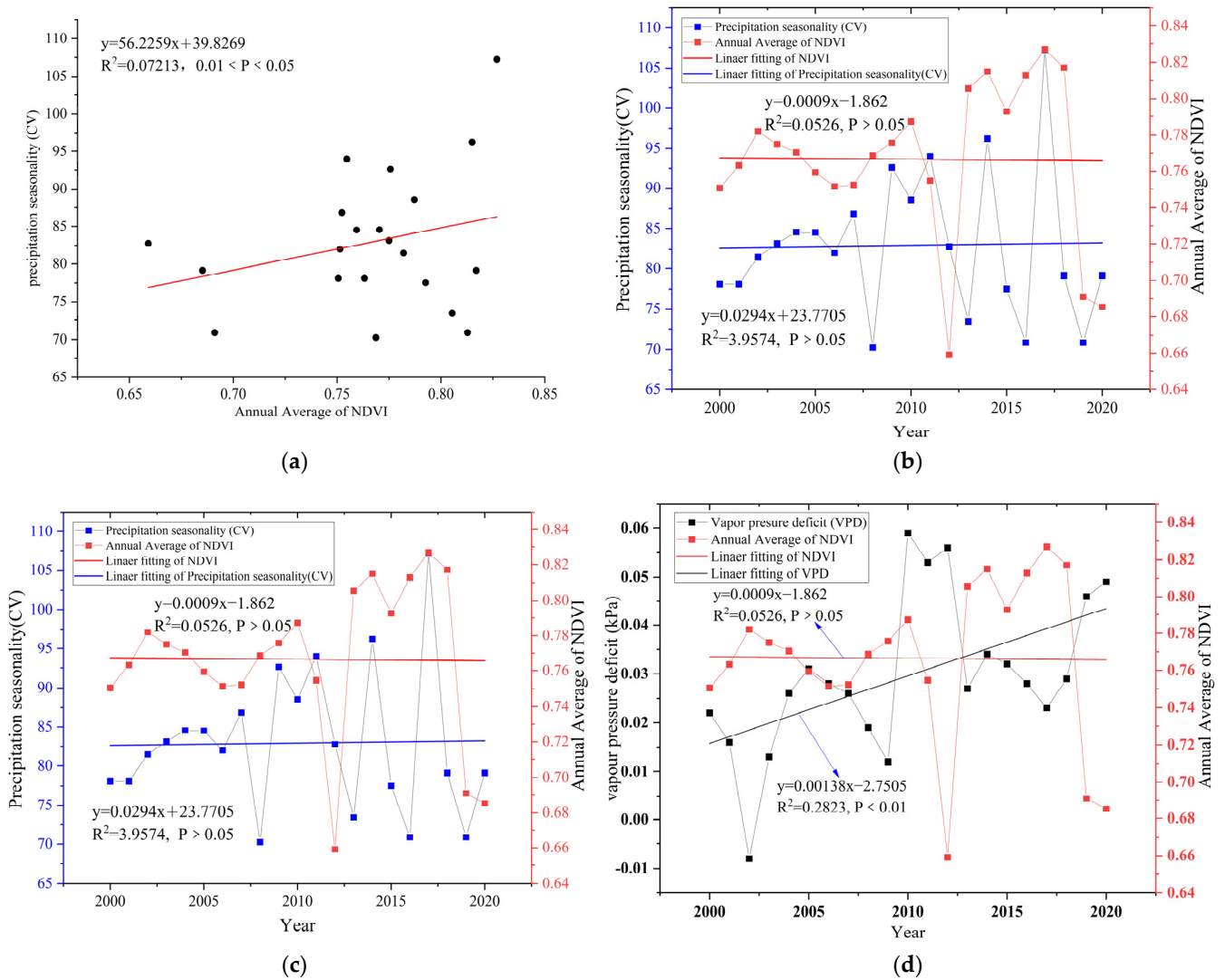
Figure 10. Variation trends and correlations of precipitation seasonality (CV), VPD, and NDVI. (**a**) Linear fitting of NDVI and precipitation seasonality (CV) trend; (**b**) Annual average change of NDVI and precipitation seasonality (CV); (**c**) Linear fitting of NDVI and VPD trend; (**d**) Annual average change of NDVI and VPD.

3.4. Detection of the Impact of Key Factors on NDVI

3.4.1. Detection Factor Influence

In order to further explore the driving characteristics of various influencing factors on the dynamic changes of Miaoling's vegetation, this section used 13 factors (Table 2) covering climate, soil, terrain, geomorphology, and human activities to conduct factor driving force and factor interaction detection on the NDVI of Miaoling's vegetation. To explore the contribution rate and interaction of climate factors and human activities to vegetation change in the Miao Mountains and further verify the differences in the main impact factors of NDVI in the Miao Mountains. The q value of the factor detection results reflects the influence of each factor on the NDVI of Miaoling's vegetation (explanatory power). The factor detection results show that the explanatory power of each factor on the NDVI is in the following order: NLI > non-karst > land use change > precipitation seasonality (CV) > karst > VPD > elevation > precipitation of the wettest quarter > MAP > slope > soil moisture > MAT > aspect. Specifically, NLI (X13) has the strongest explanatory power for NDVI (q = 0.422), and aspect (X9) has the smallest explanatory power for NDVI (q = 0.125).

The explanatory power of the above factors passed the 0.05 test with a confidence level of 95%. Overall, the explanatory power of human activities on vegetation NDVI is greater than the climactic factors in Miaoling. Additionally, the order of partial correlation and explanatory power of each factor for NDVI is consistent.

3.4.2. Detection Factor Interaction Analysis

The change in vegetation and the existence of spatial heterogeneity are driven by many factors. The interaction detection results of various influencing factors in Miaoling (Figure 11) show that their interaction is manifested as dual factor enhancement and non-linear enhancement, and all interaction factors have obvious enhancement characteristics on the driving force of NDVI compared to a single influencing factor. Among them, the interaction between land use change and NLI [q (X12∩X13) = 0.459] has the strongest explanatory power for the spatial distribution of NDVI, showing a driving feature of dual factor enhancement. On the contrary, the interaction between soil moisture and aspect orientation [q (X5∩X9) = 0.112] has the least explanatory power on NDVI. In addition, the research results also indicate that the interaction between human activity factors and other factors is significantly greater than that between other factors. It can be seen that the explanatory power of the interaction between human activities and other factors in the Miaoling area is dominant and that it is a key driving factor affecting the vegetation change in the Miaoling area.
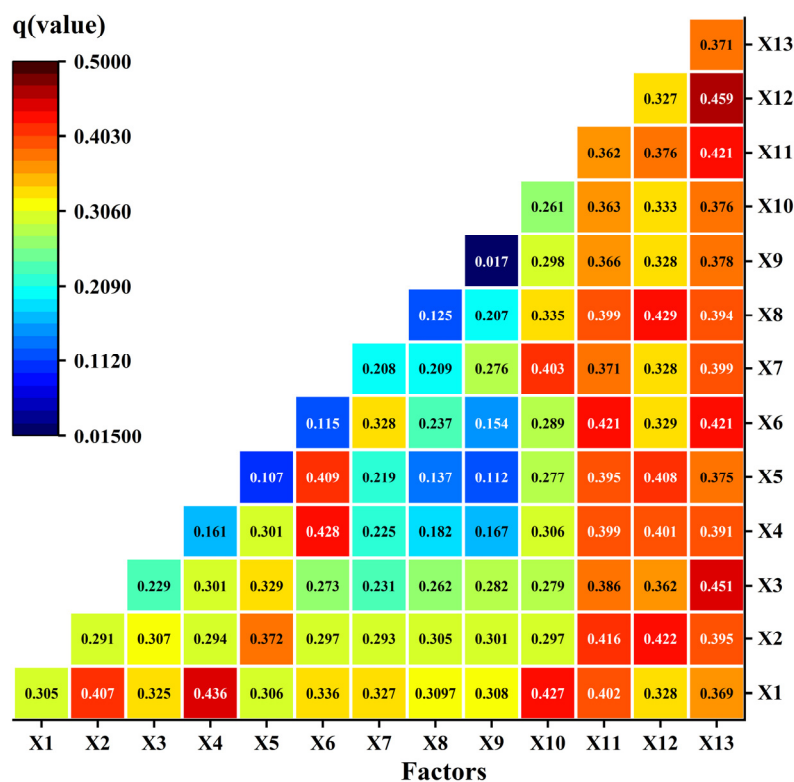

Figure 11. Explanatory power of interaction between key factors. X1, precipitation seasonality (CV); X2, VPD; X3, precipitation of wettest quarter; X4, MAP; X5, soil moisture; X6, MAT; X7, elevation; X8, slope; X9, aspect; X10, karst; X11, non-karst; X12, land use change; X13, NLI.

4. Discussion

4.1. Analysis of the Spatial Distribution Trend of NDVI

Previous research has confirmed that the ecological environment of karst regions has greatly improved [32–34,38,51–53]. Our research findings indicate that the Miaoling region has exhibited sluggish growth in NDVI over time compared to non-karst areas, indicating an improvement in their ecological environment [53,54]. This positive ecological change

is attributed to the residents' strong awareness of environmental protection as well as the preservation of subtropical evergreen broad-leaved forests, evergreen and deciduous broad-leaved mixed forests, and evergreen shrubs in the area [34,38]. Furthermore, the vegetation coverage exhibited a distribution pattern of "gradually increasing from west to east", as confirmed by an average Hurst index of 0.56. The slow and incremental increase in NDVI observed in our study area is consistent with the continuous improvement in vegetation coverage seen in other study areas across China [20–22,55]. The spatial heterogeneity of the impact of all climate factors on vegetation cover change is evident. Nevertheless, as demonstrated by Figures 6 and 7, the utilization of arable land and the increase in artificial surfaces have resulted in a consistent decline in NDVI values in the related areas.

As mentioned above, the NDVI variation in Miaoling not only shows a slow upward trend over the whole period, but there are also strong downward processes. As shown in Figure 2, NDVI declined considerably after 2010 and 2018. Notably, a considerable decrease occurred in 2012, and this phenomenon can be primarily attributed to the backdrop of global climate change, paralleling the NDVI changes seen in other karst regions of China. Investigations of this phenomenon reveal that the most severe drought and extreme weather in 50 years occurred in the karst region of southwest China in 2010 [56], leading to a sharp decline in Miaoling's NDVI that continued through 2012 and culminated in the lowest NDVI value of the entire research period. Furthermore, it is likely that the natural disasters that occurred in 2017 have had a negative impact on vegetation dynamics, thereby comprehensively influencing the overall NDVI trend in the Miaoling Mountains during the past 21 years.

4.2. NDVI Variation and Land Use Change

Human activity is widely recognized as an important driver of vegetation cover. Land use change, representing human activity, has been shown to be highly correlated with vegetation change [24,26,49,57]. Previous research studies have demonstrated the importance of land use change as a key factor in the spatial distribution of the NDVI, which significantly influences vegetation change, regional ecological security [58], and ecosystem services [59]. Our study, depicted in Figure 6b, reveals that forests in the Miaoling area have the highest NDVI value, followed by grass, shrub areas, arable land, wetland, water areas, and artificial surfaces. The changes in NDVI's distribution across different spatial and temporal scales are driven by both climatic factors and human activities [1,12,15]. The explanatory power of human activities on NDVI changes is much higher than that of climate factors, as shown in Table 4, indicating that NLI, land use change, and human activities play significant roles in the ecosystem. Land use change represent ongoing challenges for vegetation variation and the effects of anthropogenic activity [19].

The land use change characteristics of human activities in Miaoling reveal that vegetation coverage has been significantly impacted by land use change over the past 21 years. Human activities such as returning farmland to forests and grass, traditional farming practices, and the combination of human activities and climate change have played a significant role in improving or degrading the vegetation [53]. Changes in forest, arable land, and artificial land surfaces have had a considerable impact on regional vegetation coverage, primarily due to the tradeoff between forests and arable land. The distribution of land use change and changes significantly influence the NDVI's spatial distribution in the region.

4.3. Impact Climatic Factors of NDVI Variation

Understanding the relationship between regional NDVI changes and climatic factors is critical for predicting regional vegetation changes and for effective ecological restoration management [56]. Climate change affects vegetation growth and change through dynamic changes and interactions between different weather factors. Miaoling's spatial heterogeneity is evident from its correlation distributions between NDVIs and six climate factors. This is due, in part, to the spatial variability of climate change. The strongest correlation among the climatic factors is precipitation seasonality (CV), as shown in Table 3. Compared with

results from other regions, vegetation cover (0.0009/year) in the Miaoling's karst region is more sensitive to changes in climatic factors, including precipitation seasonality (CV) and VPD.

Seasonal changes in precipitation have a significant effect on NDVI, as shown by research [60]. Precipitation is the main driver of vegetation change [61]. Seasonal changes in precipitation can also influence vegetative phenology and cover [20]. In areas of high humidity, the risk of drought is lower, making the growing season of vegetation more sensitive to precipitation seasonality (CV) in order to maximize water benefits [53,55]. The results of this study show that the regularity of the temporal change of NDVI in Miaoling is similar to that of precipitation seasonality (CV) (Figure 10b). Obviously, in the period of precipitation seasonality (CV) and precipitation of the wettest quarter (i.e., plant growth season) (Figure 12a), when precipitation is abundant, with an increase in temperature to a certain extent, the photosynthesis, respiration, and transpiration processes of plants can be increased, and plant growth can be promoted. This is based on the strong precipitation seasonality in Miaoling, in the subtropical monsoon region. The rate of change of precipitation and the precipitation in the wettest season strongly promote the growing season of plants in Miaoling, and the trend of change is consistent, so it has a significant regulating effect on NDVI. NDVI is also highly positively correlated with precipitation seasonality (CV) and precipitation in the wettest season in terms of spatial heterogeneity (Figure 9a,c).
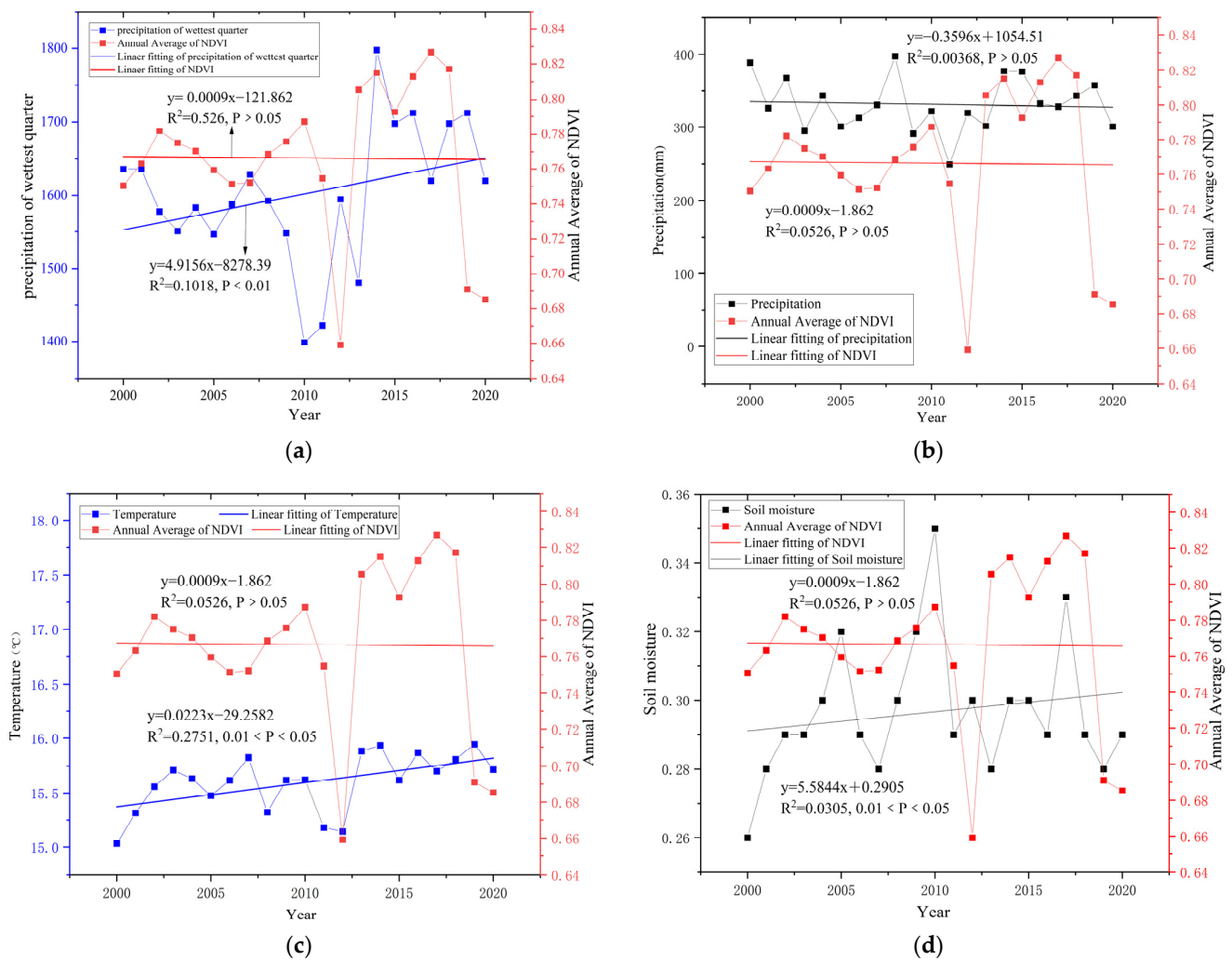

Figure 12. Time variation and trend of NDVI and precipitation of wettest quarter (**a**); MAP (**b**); MAT (**c**); soil moisture (**d**).

Furthermore, there is a significant negative correlation between VPD and NDVI, which is second only to precipitation seasonality (CV) in explaining NDVI changes. VPD also plays an important role in the interannual variability of NDVI, as an increase in VPD causes a decrease in NDVI (Figure 10c). However, current Earth system models underestimate VPD's interannual variability and its effect on GPP and NEP [50] by ignoring VPD's indirect influence on NDVI. Due to global warming, VPD is increasing, and vegetation is severely affected [55,62]. In addition, previous research has found that the vegetative landscape is "browning", i.e., plant growth is decreasing [7,63]. Above a certain threshold, plant photosynthesis and growth in most species are limited, which leads to a higher risk of hydraulic failure and a decrease in NDVI.

Temperature and precipitation are the most significant climatic drivers of vegetation growth, as per previous studies [9,11,16,20]. The change in vegetation phenology, structure, and coverage has been observed to be significant from tropical to northern regions and from coastal to inland areas [7,12,19]. However, the karst landscape, which is complex and heterogeneous, has also contributed to vegetation change, including drought and land degradation, due to rocky desertification [64,65]. The results of this study show that NDVI increases with the increase in temperature in the study time sequence (Figure 12c). The increase in temperature can increase the photosynthetic efficiency of vegetation and prolong its growth period, thereby improving the status of NDVI [6]. However, the partial correlation is slightly smaller than that of precipitation (Table 3). Contrary to the results of other studies, "temperature has a stronger impact on NDVI than precipitation" [55,64].

A study conducted on the interaction between NDVI and the climate of karst vegetation in Guizhou revealed that the effect of MAT on NDVI is stronger than that of MAP [53,60]. The study concluded that the explanatory power of MAT on NDVI in the Miaoling area is lower than that of MAP. The binary hydrological structure commonly found in karst regions leads to a substantial loss of precipitation [23], suggesting that water resources are not efficiently utilized for the thriving of vegetation. The study's findings are consistent with the fact that precipitation has a lower positive correlation with NDVI changes. This is particularly relevant in karst areas that are prone to drought, where precipitation changes have a significant impact on vegetation [34,62,66]. It is confirmed that NDVI is more sensitive to precipitation than temperature in Miaoling.

Soil moisture mainly comes from precipitation and affects vegetation growth [8,17]. Therefore, it is also one of the important factors limiting vegetation growth in karst areas. Due to the relatively thin nature of the karst soil layer, soil water is easy to lose, which limits plant growth and ecological recovery in karst areas [50,67]. In this study, the explanatory power of soil moisture is relatively weak, which also proves that the characteristics of soil moisture loss under the dual structure in karst areas are easy and the positive effect on NDVI is not significant. As shown in Figures 9e and 12d, the soil moisture of Miaoling's arable areas (mainly in non-karst areas) is highly positively correlated with NDVI, which accounts for 43.7% of Miaoling.

4.4. Influence of Factor Interaction on NDVI

Changes in vegetation growth are inextricably linked to climate variation and human activities. Based on the detection of geographical detectors, we further analyzed the interaction of 13 factors on NDVI. We found that NLI between 2000 and 2020 is the strongest driving factor for explaining the changes in vegetation in Miaoling. Additionally, the results showed that the interaction between various factors has significantly higher explanatory power for the changes in the NDVI than itself (Figure 11), which is consistent with other research results [13,16,66].

In the study, NLI has the greatest explanatory power for the trend of vegetation cover change (q = 0.422, Table 4). There are a few studies that combine NLI with NDVI, indicating that urbanization has a negative impact on vegetation coverage or the ecological environment by increasing NLI [30,68,69]. There is a significant negative correlation between vegetation coverage and NLI values. From Figures 5 and 13, it can be seen that there is

a significant overlap between the areas where NDVI continues to degrade and the areas where NLI significantly increases. The areas where NDVI improves mostly correspond to areas with a low or no nighttime light index.
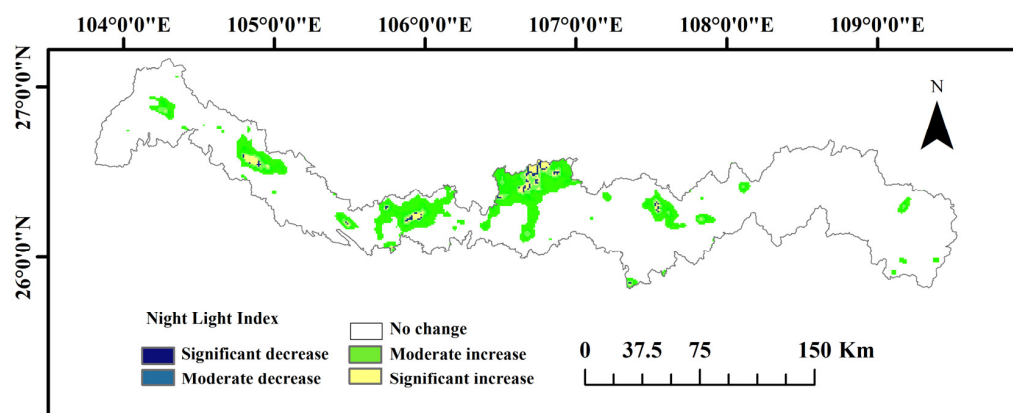

Figure 13. Characteristics and spatial distribution of NLI changes from 2000 to 2020.

Studies have shown that the interaction between precipitation seasonality (CV) (q = 0.355), land use change (q = 0.0.397), non-karst areas (q = 0.401), and NLI (q = 0.422) has the most obvious effect on the NDVI of vegetation (Table 4). Unlike other studies [5,7,43], we found that two factors of human activity and their interaction with other factors have a high explanatory power for the changes in NDVI, and it mainly shows a bifactor enhancement; the contribution rate is very large. This also shows that human activity can significantly influence the NDVI in the karst region [37,39,55]. Among them, the interaction between NLI and land use change (q (X13∩X12) = 0.459) has the largest impact on NDVI, and it mainly shows a bifactor enhancement. Therefore, human activities can be identified as the dominant factor in vegetation dynamics, while other factors only serve as constraints in karst basins. Relevant studies on the Loess Plateau have also shown this [15,20,58].

Temperature and precipitation are considered the foremost drivers of vegetation growth with regards to climatic factors, as cited by previous research [8,10,13,19]. Although the influence of mean annual temperature (MAT) (q = 0.155) and mean annual precipitation (MAP) (q = 0.21) on vegetation in Miaoling does not differ significantly, their interactions (q (X4∩X6) = 0.428) exhibit a significantly higher impact on NDVI compared to their individual effects. Furthermore, soil moisture and VPD are strongly linked to temperature and precipitation [69,70]. A few researchers have reported a direct or indirect dependence of VPD's impact on NDVI on the prevailing temperature and soil moisture conditions [25,71,72]. Hence, when the response of plants in an ecosystem decreases the evaporation capacity due to atmospheric drying, the conservation of soil moisture improves, along with some evidence of NDVI growth. This suggests that hydrothermal conditions in subtropical regions significantly influence vegetation growth and change. Moreover, the impact of factors such as altitude, slope, and aspect interaction are relatively minor in driving vegetation trends in Miaoling, but this impact increases significantly under the influence of human activities, reinforcing the crucial role of human activities in vegetation change in the Miaoling (karst area) region. In other words, the varying responses of vegetation NDVI to climate factors and human activities may be explained by the interaction of various factors in terms of temporal and spatial scale differences.

4.5. Limitations of This Study

In this study, we explored the dynamic change characteristics and trends of the regional vegetation's NDVI in Miaoling and conducted a driving analysis using climate factors, human activities, and topography. However, there are still some limitations. Firstly, we did not analyze the seasonal characteristics of vegetation growth in Miaoling, such as growing season and non-growing season. In future research, we should pay attention to

the differences between these vegetation changes and their comprehensive relationship. Secondly, due to the limitation of spatial resolution differences in NDVI and climate factors, the NDVI variation trend of some pixels may be overestimated or underestimated, as may also be found in correlation analyses. Despite these shortcomings, this work is helpful to comprehensively understand the spatiotemporal characteristics of Miaoling's vegetation and the driving factors of vegetation dynamics. At the same time, it provides a reference value for the dynamic driving factors of vegetation in important karst basins.

5. Conclusions

Based on NDVI data, the present study examines the alterations in vegetation coverage within a karst basin watershed from 2000 to 2020. Furthermore, the research also investigates the impact exerted by climate factors, topography, and human activities on Miaoling's vegetation and how they interact with each other. The key results of this study are as follows:

(1) Under the pixel scale and spatial distribution in Miaoling, the vegetation coverage gradually increases from west to east. During the study period, the NDVI of Miaoling's vegetation showed an overall upward trend (0.0009/year), with an average value of 0.766, 53.82% of the region continuing to grow, and a distribution pattern of "gradually increasing from west to east". The vegetation in NDVI showing an upward trend is much larger than the area showing a downward trend, and the site with a downward trend is mainly in the western and central parts of Miaoling.

(2) The correlation between the vegetation's NDVI and meteorological factors presents significant spatial heterogeneity. Climate change has a two-sided impact on NDVI changes in vegetation in the study area because there is a positive promoting effect and a relatively inhibitory effect for the NDVI. The NDVI and VPD of the vegetation in the study area show a negative correlation and a positive correlation with the other five climate factors as a whole, with the greatest correlation being with precipitation seasonality (CV).

(3) Compared with climate change and landform factors, human activity factors have a greater driving force on the NDVI of Miaoling's vegetation, and their interaction with other factors is also significantly higher, which also shows that the dynamic change and development trend of the NDVI of Miaoling's vegetation are strongly affected by human activities. Therefore, human activities can be considered the dominant factor driving NDVI changes in the Miaoling area.

Author Contributions: Conceptualization, Y.W. and S.L.; methodology, G.L.; software, L.G. and J.Y.; formal analysis, C.G. and F.Y.; investigation, J.Y., L.G., Z.S. and X.Y.; data curation, Y.C., H.P. and X.Y.; writing—original draft preparation, Y.W.; writing—review and editing, C.G. and S.L.; visualization, J.Y. and L.G.; supervision, Y.X.; project administration, G.L.; funding acquisition, Y.W. All authors have read and agreed to the published version of the manuscript.

Data Availability Statement: Not applicable.

Conflicts of Interest: The authors declare no conflict of interest.

References

1. Karl, T.R.; Trenberth, K.E. Modern Global Climate Change. *Science* **2003**, *302*, 1719–1723. [CrossRef] [PubMed]
2. Bonan, G.B.; Pollard, D.; Thompson, S.L. Effects of Boreal Forest Vegetation on Global Climate. *Nature* **1992**, *359*, 716–718. [CrossRef]
3. Haberl, H.; Erb, K.H.; Krausmann, F.; Gaube, V.; Bondeau, A.; Plutzar, C.; Gingrich, S.; Lucht, W.; Fischer-Kowalski, M. Quantifying and Mapping the Human Appropriation of Net Primary Production in Earth's Terrestrial Ecosystems. *Proc. Natl. Acad. Sci. USA* **2007**, *104*, 12942–12947. [CrossRef]

4. Zhang, S.R.; Bai, X.Y.; Zhao, C.; Tan, Q.; Luo, G.; Wu, L.; Xi, H.; Li, C.; Chen, F.; Ran, C.; et al. China's Carbon Budget Inventory from 1997 to 2017 and Its Challenges to Achieving Carbon Neutral Strategies. *J. Clean. Prod.* **2022**, *347*, 130966. [CrossRef]

5. Kong, D.; Miao, C.; Wu, J.; Zheng, H.; Wu, S. Time Lag of Vegetation Growth on the Loess Plateau in Response to Climate Factors: Estimation, Distribution, and Influence. *Sci. Total Environ.* **2020**, *744*, 140726. [CrossRef]

6. Piao, S.L.; Wang, X.H.; Park, T.; Chen, C.; Myneni, R.B. Characteristics, Drivers and Feedbacks of Global Greening. *Nat. Rev. Earth Environ.* **2019**, *1*, 14–27. [CrossRef]

7. Sun, Z.H.; Mao, Z.G.; Yang, L.Y.; Liu, Z.; Han, J.C.; Wanag, H.Y.; He, W. Impacts of Climate Change and Afforestation on Vegetation Dynamic in the Mu Us Desert, China. *Ecol. Indic.* **2021**, *129*, 108020. [CrossRef]

8. Liu, Y.; Li, Y.; Li, S.C.; Motesharrei, S. Spatial and Temporal Patterns of Global NDVI Trends: Correlations with Climate and Human Factors. *Remote Sens.* **2015**, *7*, 13233–13250. [CrossRef]

9. Tian, F.; Fensholt, R.; Verbesselt, J.; Grogan, K.; Horion, S.; Wang, Y.J. Evaluating Temporal Consistency of Long-Term Global NDVI Datasets for Trend Analysis. *Remote Sens. Environ.* **2015**, *163*, 326–340. [CrossRef]

10. Zheng, K.Y.; Tan, L.H.; Sun, Y.W.; Wu, Y.J.; Duan, Z.; Xu, Y.; Gao, C. Impacts of Climate Change and Anthropogenic Activities on Vegetation Change: Evidence from Typical Areas in China. *Ecol. Indic.* **2021**, *126*, 107648. [CrossRef]

11. Zhu, Z.C.; Piao, S.L.; Myneni, R.B.; Huang, M.; Zeng, Z.Z.; Canadell, J.G.; Ciais, P.; Sitch, S.; Friedlingstein, P.; Arneth, A.; et al. Greening of the Earth and its drivers. *Nat. Clim. Chang.* **2016**, *6*, 791. [CrossRef]

12. Piao, S.L.; Friedlingstein, P.; Ciais, P.; Zhou, L.M.; Chen, A.B. Effect of Climate and CO_2 Changes on the Greening of the Northern Hemisphere over the Past Two Decades. *Geophys. Res. Lett.* **2006**, *33*, 432–436. [CrossRef]

13. Rogier, D.J.; Jan, V.; Achim, Z.; Michael, S. Shifts in Global Vegetation Activity Trends. *Remote Sens.* **2013**, *5*, 1117–1133. [CrossRef]

14. Braswell, B.H.; Schimel, D.S.; Under, E.; Iii, B.M. The Response of Global Terrestrial Ecosystems to Interannual Temperature Variability. *Science* **1997**, *278*, 870–872. [CrossRef]

15. Liu, Z.J.; Wang, J.Y.; Wang, X.Y.; Wang, Y.S. Understanding the impacts of 'Grain for Green' land management practice on land greening dynamics over the Loess Plateau of China. *Land Use Policy* **2020**, *99*, 105084. [CrossRef]

16. Bogaert, J. Evidence for a Persistent and Extensive Greening Trend in Eurasia Inferred from Satellite Vegetation Index Data. *J. Geophys. Res. Atmos.* **2002**, *107*, ACL 4-1–ACL 4-14. [CrossRef]

17. Shen, M.G.; Piao, S.L.; Cong, N.; Zhang, G.G.; Jassens, I.A. Precipitation impacts on vegetation spring phenology on the Tibetan Plateau. *Glob. Chang. Biol.* **2015**, *21*, 3647–3656. [CrossRef]

18. Sun, J.; Cheng, G.; Li, W.; Sha, Y.; Yang, Y. On the Variation of NDVI with the Principal Climatic Elements in the Tibetan Plateau. *Remote Sens.* **2013**, *5*, 1894–1911. [CrossRef]

19. Zhou, X.Y.; Shi, H.D.; Wang, X.R. Impact of Climate Change and Human Activities on Vegetation Coverage in the Mongolian Plateau. *Arid Zone Res.* **2014**, *31*, 604–610. (In Chinese)

20. Shi, S.; Yu, J.; Wang, F.; Wang, P.; Zhang, Y.; Jin, K. Quantitative Contributions of Climate Change and Human Activities to Vegetation Changes over Multiple Time Scales on the Loess Plateau. *Sci. Total Environ.* **2021**, *755*, 142419. [CrossRef]

21. Zhang, B.; Wang, D.; Wang, G.G.; Qiong, M.A.; Zhang, G.B.; Ding-Min, J.I. Vegetation cover change over the southwest China and its relation to climatic factors. *Resour. Environ. Yangtze Basin.* **2015**, *24*, 956–964. (In Chinese)

22. Du, C.C.; Bai, X.Y.; Li, Y.B.; Tan, Q.; Zhao, C.W.; Luo, G.J.; Wu, L.H.; Chen, F.; Li, C.J.; Ran, C.; et al. Inventory of China's Net Biome Productivity since the 21st Century. *Land* **2022**, *11*, 1244. [CrossRef]

23. Yao, J.Q.; Li, M.Y.; Zheng, J.H. Assessing the Spatiotemporal Evolution of Anthropogenic Impacts on Remotely Sensed Vegetation Dynamics in Xinjiang, China. *Remote Sens.* **2021**, *13*, 4651. [CrossRef]

24. Guo, E.L.; Wang, Y.F.; Wang, C.L.; Sun, Z.Y.; Bao, Y.L.; Mandula, N.; Jirigala, B.; Bao, Y.H.; Li, H. NDVI Indicates Long-Term Dynamics of Vegetation and Its Driving Forces from Climatic and Anthropogenic Factors in Mongolian Plateau. *Remote Sens.* **2021**, *13*, 688. [CrossRef]

25. McDowell, N.G.; Allen, C.D. Darcy's law predicts widespread forest mortality under climate warming. *Nat. Clim. Chang.* **2015**, *5*, 669–672. [CrossRef]

26. Williams, A.P.; Allen, C.D.; Macalady, A.K. Temperature as a potent driver of regional forest drought stress and tree mortality. *Nat. Clim. Chang.* **2013**, *3*, 292–297. [CrossRef]

27. Feng, K.; Wang, T.; Liu, S.; Yan, C.; Kang, W.; Chen, X.; Guo, Z. Path analysis model to identify and analyze the causes of aeolian desertification in Mu Us Sandy Land. *China. Ecol. Indic.* **2021**, *124*, 107386. [CrossRef]

28. Liu, X.; Pei, F.; Wen, Y.; Li, X.; Wang, S.; Wu, C.; Cai, Y.L.; Wu, J.; Chen, J.; Feng, K.; et al. Global urban expansion offsets climate-driven increases in terrestrial net primary productivity. *Nat. Commun.* **2019**, *10*, 5558. [CrossRef]

29. Liu, Z.; He, C.; Zhang, Q.; Huang, Q.; Yang, Y. Extracting the dynamics of urban expansion in China using DMSP-OLS nighttime light data from 1992 to 2008. *Landse Urban Plan.* **2012**, *106*, 62–72. [CrossRef]

30. Ma, T.; Zhou, C.; Pei, T.; Haynie, S.; Fan, J. Quantitative estimation of urbanization dynamics using time series of DMSP/OLS nighttime light data: A comparative case study from China's cities. *Remote Sens. Environ.* **2012**, *124*, 99–107. [CrossRef]

31. Fu, H.; Shao, Z.; Fu, P.; Cheng, Q. The Dynamic Analysis between Urban Nighttime Economy and Urbanization Using the DMSP/OLS Nighttime Light Data in China from 1992 to 2012. *Remote Sens.* **2017**, *9*, 416. [CrossRef]

32. Zhu, S.Q.; Wei, L.M.; Chen, Z.R.; Zhang, C.G. A Preliminary Study on Biomass Components of Karst Forest in Maolan of Guizhou Province, China. *ACTA Phytoecol. Sin.* **1995**, *19*, 358. (In Chinese)

33. Liu, Y.; Liu, C.; Wang, S.; Guo, K.; Yang, J.; Zhang, X.; Li, G. Organic Carbon Storage in Four Ecosystem Types in the Karst Region of Southwestern China. *PLoS ONE* **2013**, *8*, e56443. [CrossRef]

34. Ni, J.; Luo, D.H.; Xia, J.; Zhang, Z.H.; Hu, G. Vegetation in Karst Terrain of Southwestern China Allocates More Biomass to Roots. *Solid Earth Discuss.* **2015**, *7*, 1209–1235. [CrossRef]

35. Tu, Y.L.; Yang, J. Study on biomass of the karst scrub community in central region of Guizhou province. *Carsol. Sin.* **1995**, *3*, 199–208. (In Chinese)

36. Huang, Q.H.; Cai, Y.L. Spatial Pattern of Karst Rock Desertification in the Middle of Guizhou Province, Southwestern China. *Environ. Geol.* **2007**, *52*, 1325–1330. [CrossRef]

37. Wu, Y.Y.; Liu, L.B.; Guo, C.Z.; Zhang, Z.H.; Hu, G.; Ni, J. Low carbon storage of woody debris in a karst forest in southwestern China. *Acta Geochim.* **2019**, *38*, 576–586. [CrossRef]

38. Chen, F.; Bai, X.Y.; Liu, F.; Luo, G.J.; Tian, Y.C.; Qin, L.Y.; Li, Y.; Xu, Y.; Wang, J.F.; Wu, L.H.; et al. Analysis Long-Term and Spatial Changes of Forest Cover in Typical Karst Areas of China. *Land* **2022**, *11*, 1349. [CrossRef]

39. Yang, J.L.; Dong, J.W.; Xiao, X.M.; Dai, J.H.; Wu, C.Y.; Xia, J.Y.; Zhao, G.S.; Zhao, M.M.; Li, Z.L.; Zhang, Y.; et al. Divergent Shifts in Peak Photosynthesis Timing of Temperate and Alpine Grasslands in China. *Remote Sens. Environ.* **2019**, *233*, 111395. [CrossRef]

40. Yang, J.; Huang, X. The 30 m annual land cover datasets and its dynamics in China from 1990 to 2021 [Data set]. *Earth Syst. Sci. Data* **2022**, *13*, 3907–3925. [CrossRef]

41. Peng, S.; Ding, Y.; Liu, W.; Zhi, L. 1 Km Monthly Temperature and Precipitation Dataset for China from 1901 to 2017. *Earth Syst. Sci. Data* **2019**, *11*, 1931–1946. [CrossRef]

42. Qu, L.S.; Zhu, Q.; Zhu, C.F. Monthly Precipitation Data Set with 1 km Resolution in China from 1960 to 2020. Available online: https://www.scidb.cn/en/detail?dataSetId=ff7ee051d2d44ab4a221cd810bf37251 (accessed on 18 August 2022).

43. Chen, Y.Z.; Feng, X.M.; Fu, B.J. An improved global remote-sensing-based surface soil moisture (RSSSM) dataset covering 2003–2018. *Earth Syst. Sci. Data* **2021**, *13*, 1–31. [CrossRef]

44. Fick, S.E.; Hijmans, R.J. WorldClim 2: New 1 km Spatial Resolution Climate Surfaces for Global Land Areas. *Int. J. Climatol.* **2017**, *37*, 4302–4315. [CrossRef]

45. Jiang, W.G.; Yuan, L.H.; Wang, W.J.; Cao, R.; Zhang, Y.F.; Shen, W.M. Spatio-temporal analysis of vegetation variation in the Yellow River Basin. *Eco. Indic.* **2015**, *51*, 117–126. [CrossRef]

46. Tosic, I. Spatial and Temporal Variability of Winter and Summer Precipitation over Serbia and Montenegro. *Theor. Appl. Climatol.* **2004**, *77*, 47–56. [CrossRef]

47. Correa-Díaz, A.; Romero-Sánchez, M.E.; Villanueva-Díaz, J. The greening effect characterized by the Normalized Difference Vegetation Index was not coupled with phenological trends and tree growth rates in eight protected mountains of central Mexico. *For. Ecol. Manag.* **2021**, *496*, 119402. [CrossRef]

48. Hurst, H.E. Long-Term Storage Capacity of Reservoirs. *Trans. Am. Soc. Civ. Eng.* **1951**, *116*, 770–799. [CrossRef]

49. Wang, J.F.; Zhang, T.L.; Fu, B.J. A measure of spatial stratified heterogeneity. *Ecol. Indic.* **2016**, *67*, 250–256. [CrossRef]

50. Deng, X.J.; Hu, S.; Zhan, C.H. Attribution of vegetation coverage change to climate change and human activities based on the geographic detectors in the Yellow. *Environ. Sci. Pollut. Res.* **2022**, *29*, 44693–44708. [CrossRef]

51. Yang, Q.Q.; Wang, K.L.; Zhang, C.; Yue, Y.M.; Tian, R.C.; Fan, F.D. Spatio-Temporal Evolution of Rocky Desertification and Its Driving Forces in Karst Areas of Northwestern Guangxi, China. *Environ. Geol.* **2011**, *64*, 383–393. [CrossRef]

52. Wu, L.H.; Wang, S.J.; Bai, X.Y.; Chen, F.; Li, C.J.; Ran, C.; Zhang, S.R. Identifying the Multi-Scale Influences of Climate Factors on Runoff Changes in a Typical Karst Watershed Using Wavelet Analysis. *Land* **2022**, *11*, 1284. [CrossRef]

53. Hou, W.J.; Gao, J.B.; Wu, S.H.; Dai, E.F. Interannual Variations in Growing-Season NDVI and Its Correlation with Climate Variables in the Southwestern Karst Region of China. *Remote Sens.* **2015**, *7*, 11105–11124. [CrossRef]

54. Gao, J.B.; Li, S.C.; Zhao, Z.Q.; Cai, Y.L. Investigating Spatial Variation in the Relationships between NDVI and Environmental Factors at Multi-Scales: A Case Study of Guizhou Karst Plateau, China. *Int. J. Remote Sens.* **2012**, *33*, 2112–2129. [CrossRef]

55. Zhang, W.; Zhou, L.; Zhang, Y.; Chen, Z.J.; Hu, F.N. Impacts of Ecological Migration on Land Use and Vegetation Restoration in Arid Zones. *Land* **2022**, *11*, 891. [CrossRef]

56. Muradyan, V.; Tepanosyan, G.; Asmaryan, S.; Saghatelyan, A.; Dell'Acqua, F. Relationships between NDVI and climatic factors in mountain ecosystems: A case study of Armenia. *Remote Sens. Appl. Soc. Environ.* **2019**, *14*, 158–169. [CrossRef]

57. Snyder, K.A.; Tartowski, S.L. Multi-Scale Temporal Variation in Water Availability: Implications for Vegetation Dynamics in Arid and Semi-Arid Ecosystems. *J. Arid Environ.* **2006**, *65*, 219–234. [CrossRef]

58. Fu, B.J.; Wang, S.; Liu, Y.B.; Liu, J.; Liang, W.; Miao, C.Y. Hydrogeomorphic Ecosystem Responses to Natural and Anthropogenic-Changes in the Loess Plateau of China. *Annu. Rev. Earth Planet. Sci.* **2016**, *45*, 223–243. [CrossRef]

59. Cairns, J.J. Ecosystem Services: An Essential Component of Sustainable Use. *Environ. Health Perspect.* **1995**, *103*, 534. [CrossRef]

60. Ma, S.B.; An, Y.L.; Yang, G.; Zhang, Y. The Analysis of the Difference Vegetation Variation and Driver Factors on NDVI Change in Karst Region: A Case on Guizhou. *Ecol. Environ. Sci.* **2016**, *25*, 1106–1114. [CrossRef]

61. Hua, W.J.; Chen, H.S.; Zhou, L.M.; Xie, Z.H.; Qin, M.H.; Li, X.; Ma, H.D.; Huang, Q.H.; Sun, S.L. Observational quantification of climatic and human influences on vegetation greening in China. *Remote Sens.* **2017**, *9*, 425. [CrossRef]

62. He, B.; Chen, C.; Lin, S.G.; Yuan, H.W.; Chen, D.L.; Zhang, Y.F.; Guo, L.L.; Zhao, X.; Liu, X.B.; Piao, S.L.; et al. Worldwide impacts of atmospheric vapor pressure deficit on the interannual variability of terrestrial carbon sinks. *Natl. Sci. Rev.* **2022**, *9*, nwab150. [CrossRef] [PubMed]

63. Du, X.L.; Wang, S.J. Space-time distribution of soil water in a karst area: A case south of the Wangjiazhai catchment, Qingzhen, Guizhou province. *Earth Environ.* **2008**, *3*, 193–201. (In Chinese)

64. Bai, X.Y.; Wang, S.J.; Xiong, K.N. Assessing spatial temporal evolution processes of karst rocky desertification land: Indications for restoration strategies. *Land Degrad. Dev.* **2013**, *24*, 47–56. [CrossRef]

65. Yan, X.; Cai, Y.L. Multi-scale anthropogenic driving forces of karst rocky desertification in southwest China. *Land Degrad. Dev.* **2015**, *26*, 193–200. [CrossRef]

66. Deng, Y.H.; Wang, S.J.; Bai, X.Y.; Luo, G.J.; Tian, S.Q. Characteristics of Soil Moisture Storage from 1979 to 2017 in the Karst Area of China. *Geocarto Int.* **2019**, *36*, 903–917. [CrossRef]

67. Yang, X.D.; Ali, A.; Xu, Y.L.; Jiang, L.M.; Lv, G.H. Soil Moisture and Salinity as Main Drivers of Soil Respiration across Natural Xeromorphic Vegetation and Agricultural Lands in an Arid Desert Region. *Catena* **2019**, *177*, 126–133. [CrossRef]

68. Li, S.X.; Wu, Q. Effects of China's ecological restoration on economic development based on Night-Time Light and NDVI data. *Environ. Sci. Pollut. Res.* **2021**, *28*, 65716–65730. [CrossRef]

69. Xu, B.; Lin, B. How industrialization and urbanization process impact on CO_2 emissions in China: Evidence from nonparametric additive regression models. *Energy Econ.* **2015**, *48*, 188–202. [CrossRef]

70. Massmann, A.; Gentine, P.; Lin, C. When does vapor pressure deficit drive or reduce evapotranspiration? *J. Adv. Model Earth Syst.* **2019**, *11*, 3305–3320. [CrossRef]

71. Fu, Z.; Ciais, P.; Prentice, I.C.; Gentine, P.; Makowski, D.; Bastos, A.; Luo, X.Z.; Green, J.K.; Stoy, P.C.; Yang, H.; et al. Atmospheric dryness reduces photosynthesis along a large range of soil water deficits. *Nat. Commun.* **2022**, *13*, 989. [CrossRef] [PubMed]

72. Humphrey, V.; Berg, A.; Ciais, P.; Gentine, P.; Jung, M.; Reichstein, M.; Seneviratne, S.I.; Frankenberg, C. Soil moisture–atmosphere feedback dominates land carbon uptake variability. *Nature* **2021**, *592*, 65–69. [CrossRef] [PubMed]